

Calibration of the mechanism based method SLaMA against NLFEA for URM detached houses

Cross-validation and calibration of simplified methods for different building typologies

Tavus, A.; Longo, M.; Messali, F.

Publication date

2020

Document Version

Final published version

Citation (APA)

Tavus, A., Longo, M., & Messali, F. (2020). *Calibration of the mechanism based method SLaMA against NLFEA for URM detached houses: Cross-validation and calibration of simplified methods for different building typologies*. Delft University of Technology.

Important note

To cite this publication, please use the final published version (if applicable).
Please check the document version above.

Copyright

Other than for strictly personal use, it is not permitted to download, forward or distribute the text or part of it, without the consent of the author(s) and/or copyright holder(s), unless the work is under an open content license such as Creative Commons.

Takedown policy

Please contact us and provide details if you believe this document breaches copyrights.
We will remove access to the work immediately and investigate your claim.

<i>Project number</i>	TC19/20
<i>File reference</i>	TC19/20-R02
<i>Date</i>	7 March 2020
<i>Corresponding author</i>	Francesco Messali (f.messali@tudelft.nl)

Cross-validation and calibration of simplified methods for different building typologies

CALIBRATION OF THE MECHANISM-BASED METHOD SLAMA AGAINST NLFEA FOR URM DETACHED HOUSES

Authors: Ahmet Tavus, Michele Longo, Francesco Messali

Cite as: *Tavus, A., Longo, M., Messali, F. Calibration of the mechanism-based method SLAMA against NLFEA for URM detached houses. Report no. TC19/20-R02, Version 01, 7 March 2020. Delft University of Technology*

This document is made available via the website 'Structural Response to Earthquakes' and the TU Delft repository. While citing, please verify if there are recent updates of this research in the form of scientific papers.

All rights reserved. No part of this publication may be reproduced, stored in a retrieval system of any nature, or transmitted, in any form or by any means, electronic, mechanical, photocopying, recording or otherwise, without the prior written permission of TU Delft.

TU Delft and those who have contributed to this publication did exercise the greatest care in putting together this publication. This report will be available as-is, and TU Delft makes no representations of warranties of any kind concerning this Report. This includes, without limitation, fitness for a particular purpose, non-infringement, absence of latent or other defects, accuracy, or the presence or absence of errors, whether or not discoverable. Except to the extent required by applicable law, in no event will TU Delft be liable for on any legal theory for any special, incidental consequential, punitive or exemplary damages arising out of the use of this report.

This research work was funded by the Dutch Ministry of Economic Affairs and Climate Policy (Ministerie van Economische Zaken en Klimaat; EZK), under the contract number 1300030718.

Table of Contents

1	Introduction.....	3
2	Description of the reference buildings	4
2.1	EUC-BUILD-2.....	4
2.2	LNEC-BUILD-3	5
3	Set of variations used for the cross-comparison study.....	6
3.1	Complete Buildings	6
3.1.1	EUC-BUILD-2.....	6
3.1.2	LNEC-BUILD-3	7
3.2	Single façade.....	8
i.	Number and size of the openings	8
ii.	Position of the openings	9
iii.	Height of the spandrels	9
iv.	Masonry type.....	9
v.	Wall thickness	9
vi.	Floor type	9
vii.	Distribution of lateral loads	9
4	Methodology used for SLaMA and NLFEA.....	11
4.1	SLaMA models	11
4.2	Finite Elements models in Diana 10.3.....	12
5	Comparison of the results	14
5.1	3D analyses.....	14
5.1.1	EUC-BUILD-2.....	14
5.1.2	LNEC-BUILD-3	17
5.2	2D analyses.....	23
6	Conclusions	29
	References.....	30

1 Introduction

The work described in the current document is part of the project “Cross-validation and calibration of simplified methods for different building typologies”, which aims at the calibration of simplified models against more sophisticated nonlinear finite element analyses (NLFEA) for specific building typologies. Namely, the project focuses on the calibration of the mechanism-based analyses (SLaMA method) against full NLFEA for nonlinear pushover (NLPO) analyses.

In the proposal document of the project [1], three specific building groups are identified: (i) terraced and semi-detached houses; (ii) detached houses; (iii) farmhouses. The work described in this document is limited to the first building group, detached houses.

The proposal document identifies buildings EUC-BUILD-2 and LNEC-BUILD-3 as reference buildings. The two buildings were tested in dynamic conditions on a shake table at the laboratories of EUCENTRE (Pavia, Italy) and LNEC (Lisbon, Portugal). A short description of buildings EUC-BUILD-2 and LNEC-BUILD-3 is provided in Section 2, and more details are available in the original testing reports [2] and [3]. The comparison between the different analyses focuses on the equivalent bilinear curve, and especially on the following parameters: (i) the initial stiffness K_{ini} ; (ii) the base shear capacity V_{bi} ; (iii) the displacement capacity d_{NC} . The present work aims eventually to identify and recommend possible correction (“model”) factors that, when applied to the results of the simplified methods, may allow to get results in line with those obtained via more sophisticated NLFEA.

Since two analyses are not enough to consider adequately the variations of the detached houses, an extensive sensitivity study is carried out to complement the research. Along with the analysis of the complete buildings, also 2D analyses of single façades are performed in order to investigate the origin of the differences in terms of structural in-plane capacity between the results obtained with simplified and sophisticated analyses. A description of all the variations is provided in Section 3.

The methodology followed to simulate the structural behaviour with the NLFEA and the SLaMA method is summarised in Section 4. A comparison between the results obtained with the two analyses is presented in Section 5. The conclusive remarks with the proposal of the model factors can be found in Section 6.

2 Description of the reference buildings

As introduced in Section 1, in order to capture the high variability between detached houses, the study presented in this report refers to two different reference buildings as starting models to introduce the variations in terms of geometry, materials and loading.

A description of the two original case studies is presented in the next sections.

2.1 EUC-BUILD-2

The first case study refers to a specimen tested on a shake table at the laboratory of EUCENTRE (Pavia, Italy) and named EUC-BUILD-2 [2]. The specimen was designed to resemble typical one-storey detached houses with a pitched roof (Figure 1), it was composed of a first-floor timber diaphragm and of a pitched timber roof finished with clay tiles. Double-wythe masonry walls supported the floor and roof framing members, and extended above the first floor to form gables at the front (north) and back (south) of the building, as shown in Figure 2. More details about the considered specimen are provided in the testing report [2].



Figure 1: Buildings with construction details similar to those adopted for the shake-table test specimen (from [2]), and actual specimen tested at the laboratory of Eucentre (from [4]).

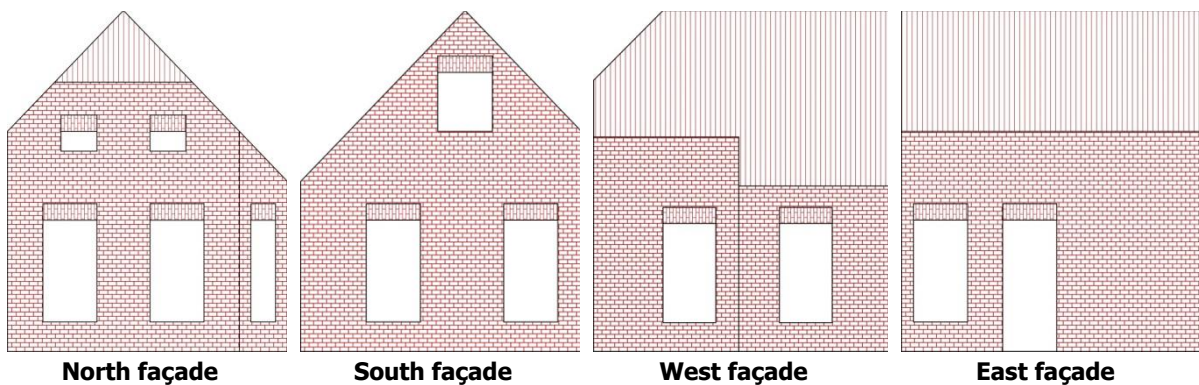


Figure 2: Layout of the façades of reference building EUC-BUILD-2, as studied in the current work.

2.2 LNEC-BUILD-3

Similarly to the first reference case, the second case study considers a specimen, named LNEC-BUILD3, which was tested on a shake table at the laboratory facilities of the Laboratório Nacional de Engenharia Civil (LNEC, Lisbon, Portugal) [3]. Also this specimen was built to resemble a typical pre-1940 Dutch detached house in the Groningen area (Figure 3). As shown in Figure 4, the specimen was composed of a high symmetrical gambrel roof finished with clay tiles; a vertical chimney was found on the west façade. The east and the west walls extended above the timber floor in gables, weakly connected to the floor and the roof framing. The load-bearing structural system consisted of 208 mm thick double-wythe clay URM walls in three out of the four perimeter walls. A 100 mm thick interior wall was built parallel to the shaking direction, longwise the centreline of the building plan. The east façade consisted of single wythe wall with 10cm thickness.

More details about the considered specimen are provided in the testing report



Figure 3: Building views, a) North-East view, b) South-East view (from [3]).

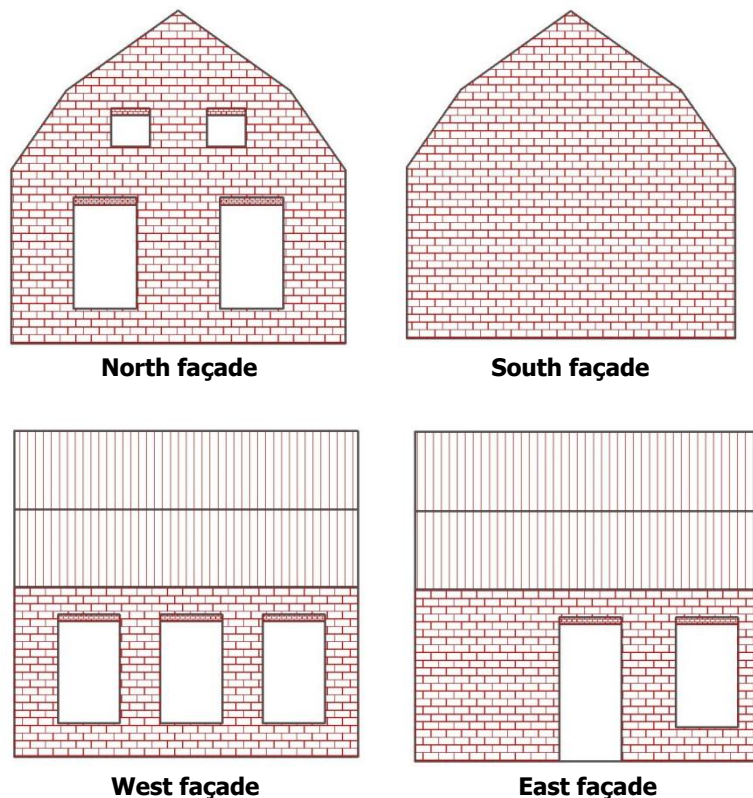


Figure 4: Layout of the façades of reference building LNEC-BUILD-3, as studied in the current work

3 Set of variations used for the cross-comparison study

The current project aims to compare the results of FEM NLPO analyses performed with DIANA FEA 10.3, with those computed following the SLaMA method for a generic detached house. For this reason, a number of variations are introduced consistently to the two reference buildings, and the comparison is performed for each of these variations. In addition, the variations of a single façade (the original East façade of EUC-BUILD-2) are studied in order to determine where the difference with the results obtained by the more sophisticated analyses come from: whether from the assessment of a 2D perforated wall or from other points, such as the connection with the transversal walls (i.e. the flange effect) or the redistribution of forces between the façades.

All the variations which were used to investigate the differences between both methods are reported hereafter.

3.1 Complete Buildings

3.1.1 EUC-BUILD-2

All variations were analysed for both positive (North/South) and negative (South/North) loading direction. Only a uniform lateral load distribution was considered. In total, sixteen different validations were evaluated. The following variations were considered:

- 1. Building plan regularity:** Three different plan configurations are considered: the original building plan (P1), rectangular shape (P2), and re-entrant corner twice longer than the original one (P3) (Figure 5);

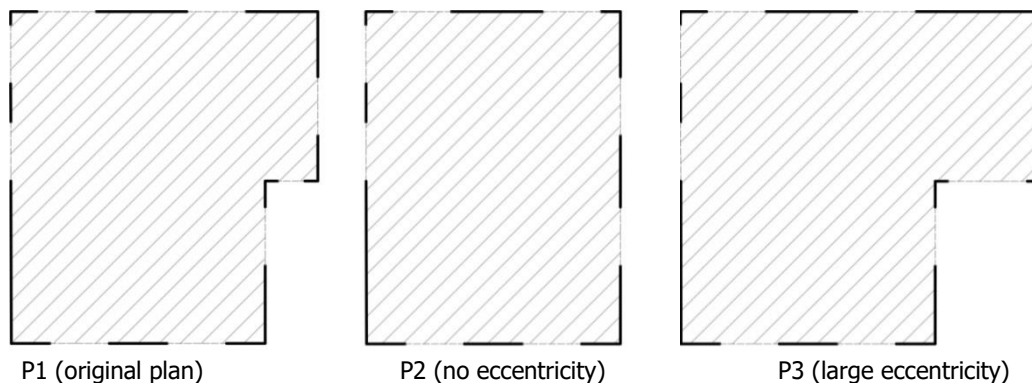


Figure 5: Building plan regularities

- 2. Openings on the East façade:** Three different layouts of the east façade variations are considered, as shown Figure 6;

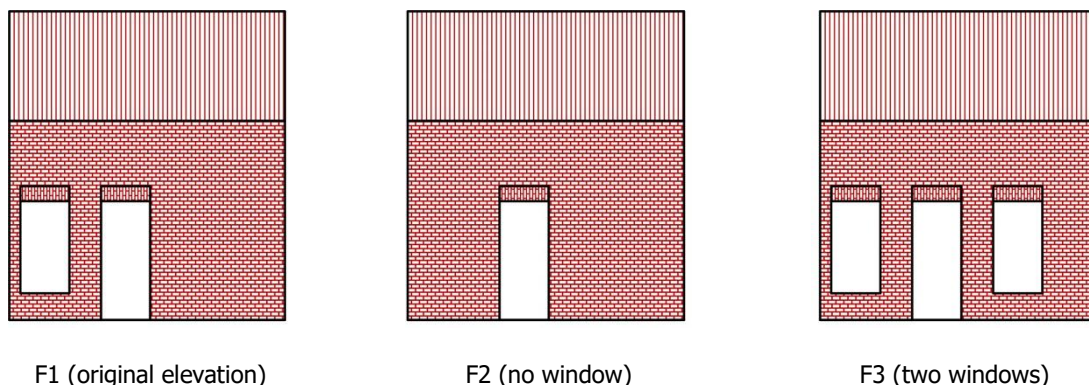


Figure 6: Variations of the East façade

- 3. Material properties:** Two URM types are considered: Solid clay bricks with general purpose mortar pre-1945 (CL1) and post-1945 (CL2). The material properties are defined according to Table F.2 of NPR 9998.

- 4. Wall thickness :** Both single-whyte (SW) and double-whyte (DW) walls are considered for both masonry types.

A total of 16 variations is then obtained, as summarised in Table 1.

Table 1. Variations considered in this study for EUC-BUILD-2. The variations are reported for the positive loading direction only; for the negative loading direction, the same variations are considered.

No.	Name	Plan regularity	Façade openings	Masonry type	Wall thickness	Loading direction
#01	P1/F1/CL1/DW/NS/U	P1	F1	CL1	DW	North/South
#02	P2/F1/CL1/DW/NS/U	P2	F1	CL1	DW	North/South
#03	P3/F1/CL1/DW/NS/U	P3	F1	CL1	DW	North/South
#04	P1/F2/CL1/DW/NS/U	P1	F2	CL1	DW	North/South
#05	P1/F3/CL1/DW/NS/U	P1	F3	CL1	DW	North/South
#06	P1/F1/CL2/DW/NS/U	P1	F1	CL2	DW	North/South
#07	P1/F1/CL1/SW/NS/U	P1	F1	CL1	SW	North/South
#08	P1/F1/CL2/SW/NS/U	P1	F1	CL2	SW	North/South

3.1.2 LNEC-BUILD-3

All variations were analysed for both positive (East/West) and negative (West/East) loading direction. Only a uniform lateral load distribution was considered. In total, sixteen different validations were evaluated. The following variations were considered:

All variations were analysed out both positive (North/South) loading direction and negative direction (South/North) by both SLaMA and NLFEA. Totally 30 different validations were evaluated. To evaluate differences between SLaMA and NLFEA, the SLaMA approach is compared NLFEA and both methods critiqued in this study.

- 1. Openings on the North façade:** Three different layouts of the openings on the north façade, with different opening percentages and eccentricities, are considered, as shown Figure 7.

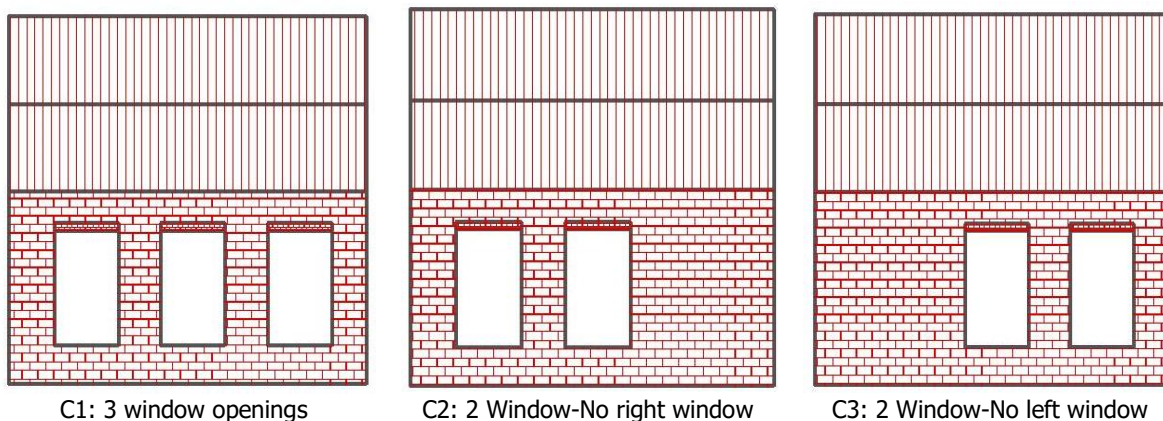


Figure 7: Variation of the North façade

- 2. Internal Wall Length:** Three different variations of the length of the internal wall are considered, as shown in Figure 8.

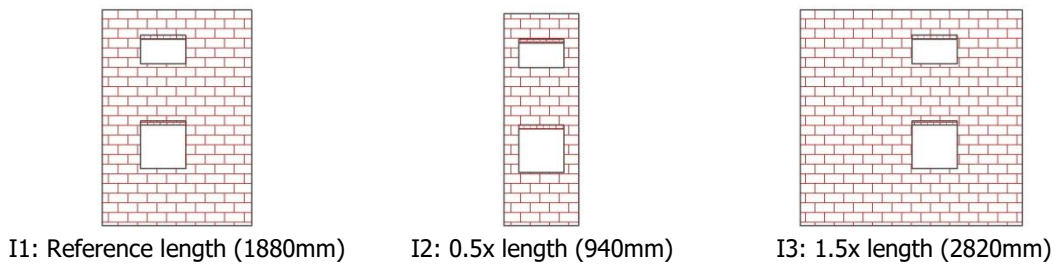


Figure 8: Interior wall length variations

3. **Wall thickness:** Three different combinations of the wall thickness are considered: (i) the original thickness (DW for North, South and West façades; SW for East façade); (ii) DW for all walls; (iii) SW for all walls.
4. **Material properties:** Two URM types are considered: Solid clay bricks with general purpose mortar pre-1945 (CL1) and post-1945 (CL2). The material properties are defined according to Table F.2 of NPR 9998.
5. **Bond type:** Two different types of bond pattern used which are: the Dutch Bond (DB) (as for the reference case) and the Running Bond (or stretcher) (RB). It should be noted that this variation has no effect of the analyses carried out with SLaMA.

A total of 30 variations is then obtained, as summarised in Table 2.

Table 2. Variations considered in this study for LNEC-BUILD-3. The variations are reported for the positive loading direction only; for the negative loading direction, the same variations are considered.

No.	Name	Façade openings	Internal wall length	Wall thickness	Material properties	Loading direction
#1	C1/I1/RW/CL2/DB/EW/U	C1	I1	Original	CL2	East/West
#2	C1/I1/RW/CL1/DB/EW/U	C1	I1	Original	CL1	East/West
#3	C1/I1/SW/CL2/DB/EW/U	C1	I1	SW	CL2	East/West
#4	C1/I1/SW/CL1/DB/EW/U	C1	I1	SW	CL1	East/West
#5	C1/I1/DW/CL2/DB/EW/U	C1	I1	DW	CL2	East/West
#6	C1/I2/RW/CL2/DB/EW/U	C1	I2	Original	CL2	East/West
#7	C1/I3/RW/CL2/DB/EW/U	C1	I3	Original	CL2	East/West
#8	C2/I1/RW/CL2/DB/EW/U	C2	I1	Original	CL2	East/West
#9	C2/I1/RW/CL1/DB/EW/U	C2	I1	Original	CL1	East/West
#10	C2/I1/SW/CL2/DB/EW/U	C2	I1	SW	CL2	East/West
#11	C2/I1/SW/CL1/DB/EW/U	C2	I1	SW	CL1	East/West
#12	C3/I1/RW/CL2/DB/EW/U	C3	I1	Original	CL2	East/West
#13	C3/I1/RW/CL1/DB/EW/U	C3	I1	Original	CL1	East/West
#14	C3/I1/SW/CL2/DB/EW/U	C3	I1	SW	CL2	East/West
#15	C3/I1/SW/CL1/DB/EW/U	C3	I1	SW	CL1	East/West

3.2 Single façade

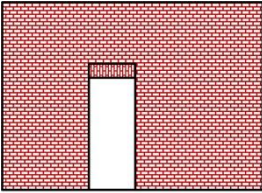
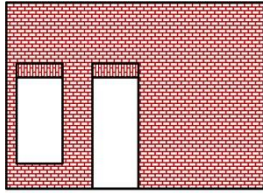
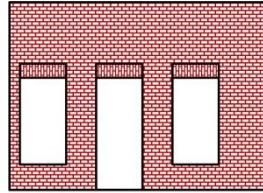
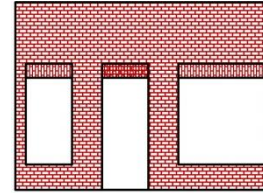
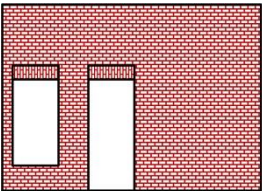
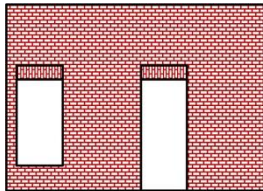
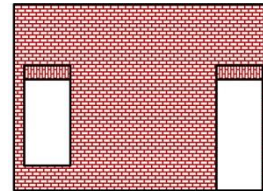
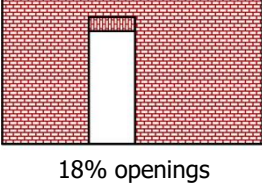
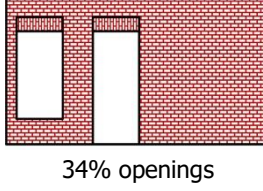
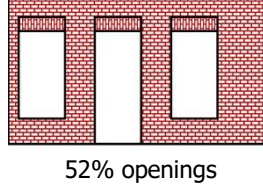
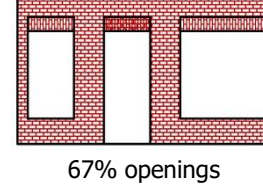
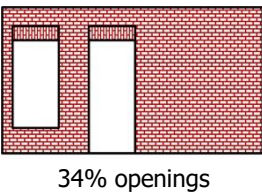
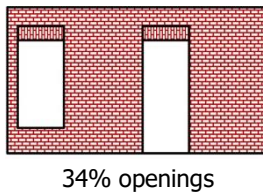
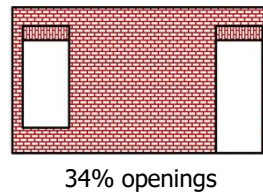
For the 2D analyses of a façade, the East façade of the EUC-BUILD-2 building is considered. Given the lower computational effort, for the 2D analyses all the variations are combined systematically and a much larger total number of combinations is then obtained (576 combinations are analysed).

The following variations are considered:

- i. **Number and size of the openings.** In addition to the reference case three variations are considered (Table 3): the removal of the existing window and the addition of a second window (either of the same dimension of the original, or larger). Four different opening percentage are then obtained: 18%, 34%, 52% and 67%.

- ii. **Position of the openings.** The position of the main door is varied in three different positions (Table 3) to assess the influence of the length of each single pier for the same opening percentage.
- iii. **Height of the spandrels.** The original building is characterized by very high spandrels, so that a weak pier-strong spandrel mechanism is expected to develop for every variation. Shorter spandrels (Table 3) are then consider to assess the influence of the spandrels on the overall resistance of the wall.
- iv. **Masonry type.** Both solid clay bricks with general purpose mortar pre- and post-1945 are considered.
- v. **Wall thickness.** Both double-wythe and single-wythe walls (that represent the inner load-bearing leaf of a cavity wall) are considered for both the masonry types.
- vi. **Floor type** Two set of properties for the timber floors are considered, with different flexibility of the diaphragm that allows larger or smaller force redistribution between the different walls.
- vii. **Distribution of lateral loads.** Three different types of lateral load distributions are considered. In addition to the standard uniform and modal patterns distributed proportionally to the mass along the height of the façade, also a distribution with the lateral load applied only at the floor level is modelled. This additional distribution is in fact that commonly used with the SLaMA method and allows for a more straightforward comparison with the NLFEA.

Table 3. Graphical representation of the variations of the geometry of the East façade of the analysed building

High spandrels	No. and size of openings	 18% openings	 34% openings	 52% openings	 67% openings
	Position of the openings	 34% openings	 34% openings	 34% openings	-
Short spandrels	No. and size of openings	 18% openings	 34% openings	 52% openings	 67% openings
	Position of the openings	 34% openings	 34% openings	 34% openings	-

The following notation is used: to define the façade layout:

- C1: Reference Case - 34% Openings - Door on the left - One Window
- C2: 34% Openings - Mid Door - One Window
- C3: 34% Openings - Right Door - One Window
- C4: 18% Openings - Door on the left – No windows
- C5: 52% Openings - Door on the left - Two window with same width
- C6: 67% Openings - Door on the left - Two window with different width

4 Methodology used for SLaMA and NLFEA

4.1 SLaMA models

The SLaMA analyses are performed according to the procedure and the equations recommended in Annex G of NPR 9998:2018 [5]. Each analysis follows the following steps:

1. Each perforated wall (i.e. each façade) is divided into single elements. The meshing procedure follows the recommendations reported in Section G.9.2.1, based on the identification of the compressive struts in the walls (Figure 9a). An example of the mesh of the east façade is presented in Figure 9b, where the piers of the storey are conservatively assumed to be cantilever or double clamped due to structural conditions of stiff or flexible floor.
2. The vertical loads acting on each piers and contributing to the structural stability are computed, based on the initial static configuration and taking into account possible flanges.
3. The force-displacement behaviour of each pier is computed. The second order effects are taken into account as reported in Section 4.4.2.2 of NPR 9998:2018 [5].
4. The capacity of each single façade is evaluated separately (wall line capacity). That is computed by summing up the capacity of the individual members of that wall (Figure 10).
5. The capacity in terms of normalized accelerations is computed for each wall by scaling the force capacity by the effective mass associated to that wall.
6. The wall with the minimum normalized capacity is governing for the whole structure, since no force redistribution between different walls is assumed to be possible due to the flexible floor.
7. The capacity of the structure is then computed for the whole building by scaling the normalized capacity of the governing wall by the total effective mass of the building.
8. The equivalent bilinear curve is computed in accordance with the recommendations of Section G.4.2 of NPR 9998:2018 [5].

For the single wall, the capacity is determined directly at point 4, and then the equivalent bilinear curve is computed.

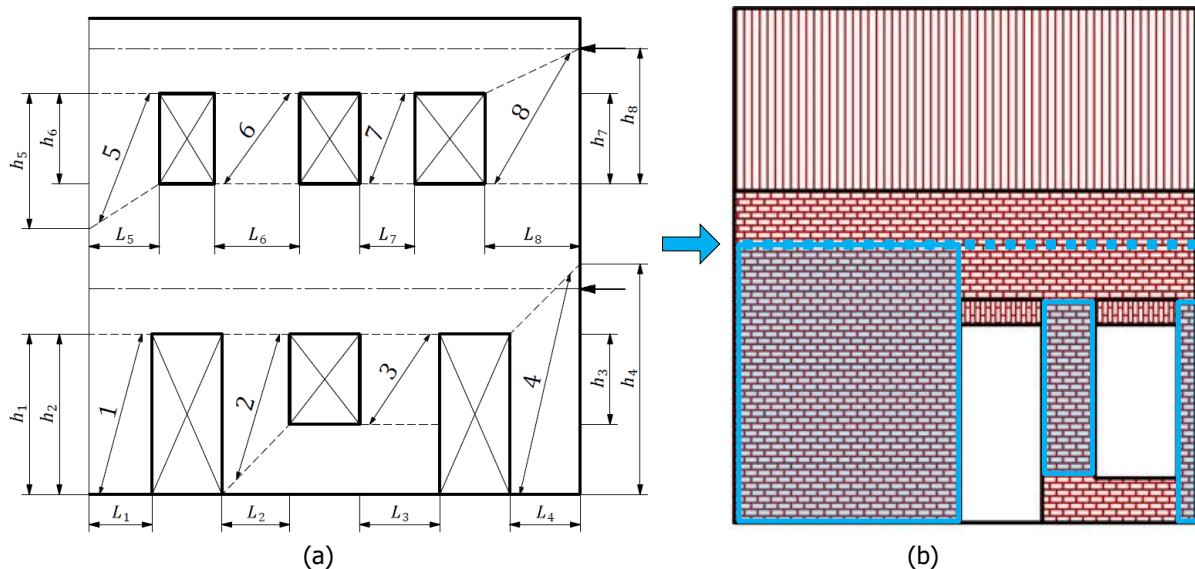


Figure 9: Graphical representation of the compressive struts of a perforated wall as recommended in [5] (a), and example of meshing on the West façade of the reference building (b). The dashed line represents the floor level.

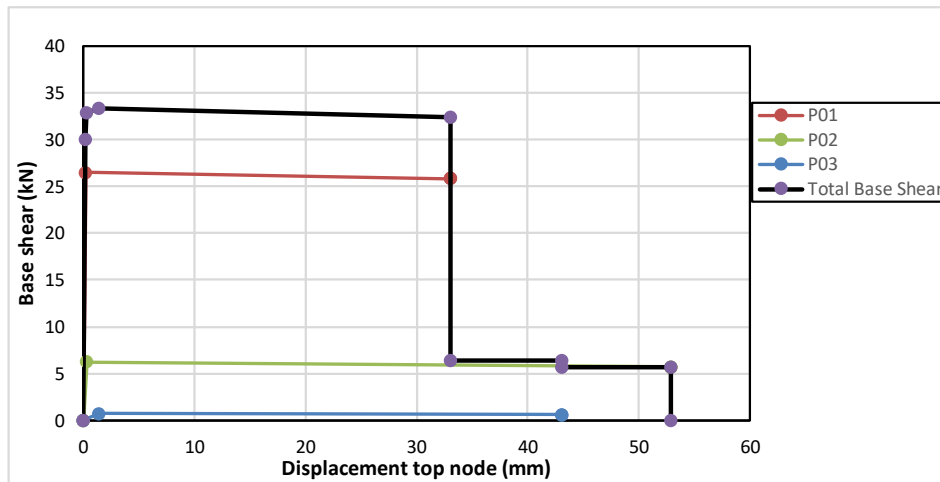


Figure 10: Example of capacity curve of piers for the east façade of EUC-BUILD-2

4.2 Finite Elements models in Diana 10.3

The detached houses representing the variations of either EUC-BUILD-2 or LNEC-BUILD-3, and of the single walls are numerically modelled in 2D and 3D by the software Diana 10.3. Quadratic 8-noded curved shell elements (CQ40S and CT30S) are used to model walls, floors of the 3D building. The irregular and complex roof and floor framings, made by timber beams, are modelled with linear Class-III beam element (CL18B). A non-linear constitutive behaviour is considered for the masonry walls, while the rest of the elements are linear elastic. The Engineering Masonry Model is selected as material model for the two different clay masonry types (before and after 1945). The material properties of masonry are taken from Table F.2 of NPR 9998:2018 [5]. An orthotropic behaviour, whose properties are calibrated according to the laboratory experiment, is assigned to timber planks of the floor and the roof. Reduced stiffness properties are assigned to a second variation of timber floor. Mass densities are selected in order to match the experimental specimen mass. The model is restrained at the bottom from translations and rotations. The elements are meshed with an average size of 200x200 mm (two examples of the mesh used for case study #01 of EUC-BUILD-2 and LNEC-BUILD-3, respectively, are depicted in Figure 11 and Figure 12). Unlike the 3D models, the approach for the 2D models makes use of quadratic 8-noded plane stress elements (CQ16M and CT12M) to model the East façade. The elements corresponding to the floors are modelled with a fictitious thickness (1 m) such that the higher stiffness compared to the walls is taken into account. The mass density of these elements is adapted to consider the actual gravity loads acting on the walls.

The applied vertical loading at floor and roof level, is directly taken from 3D model. The mesh size is reduced to 100x100 mm. Two examples of meshes 2D models are depicted in Figure 13.

Non-linear static analyses are performed for both 2D and 3D models. The model is initially subjected to the gravity loads in ten equal steps. Then, either uniform distributed lateral loads, applied via a uniform lateral acceleration, or modal distributed lateral loads, based on the main eigen-mode (and the corresponding participating mass) of the structure obtained via eigen-value analyses, is applied such that an average displacement rate of 0.1 mm/step is recorded at floor level. The Secant BFGS (Quasi-Newton) method is adopted as iterative method in combination with the Arc-Length control. Both displacement and force norms must be satisfied during the iterative procedure within a tolerance of 1%. The Parallel Direct Sparse method is employed to solve the system of equations. The second order effects are considered via the Total Lagrange geometrical nonlinearity.

The force-displacement curve of the building is extrapolated at floor level and the equivalent bilinear curve is computed according to the procedure recommended in Section G.4.2 of NPR 9998:2018 [5] and summarised for the SLaMA method.

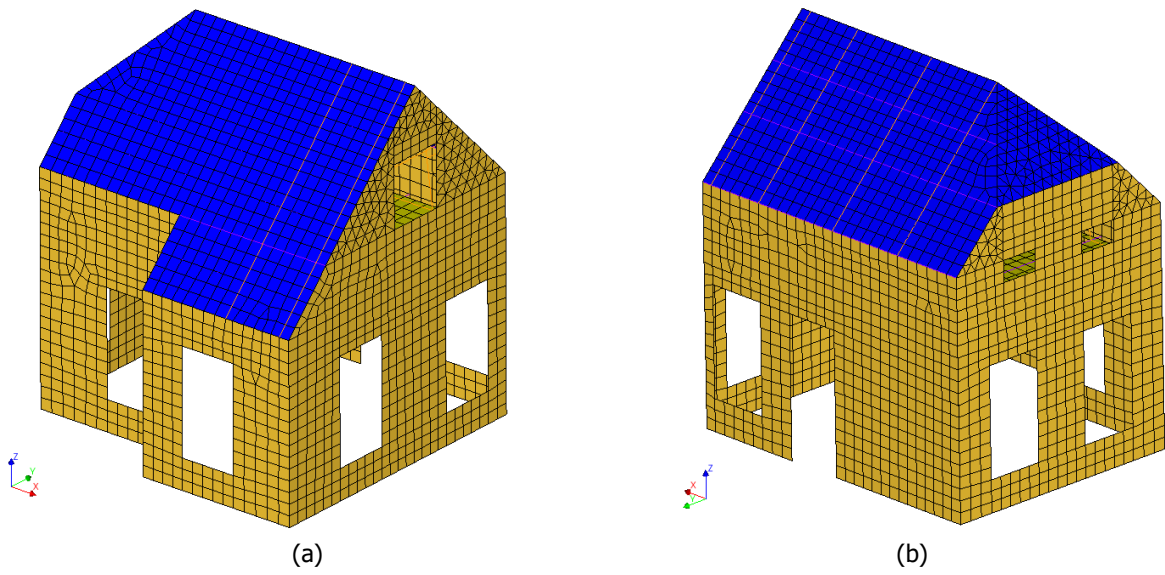


Figure 11: 3D model of EUC-BUILD-2, variation #01. South-West view (a) and North-East view (b).

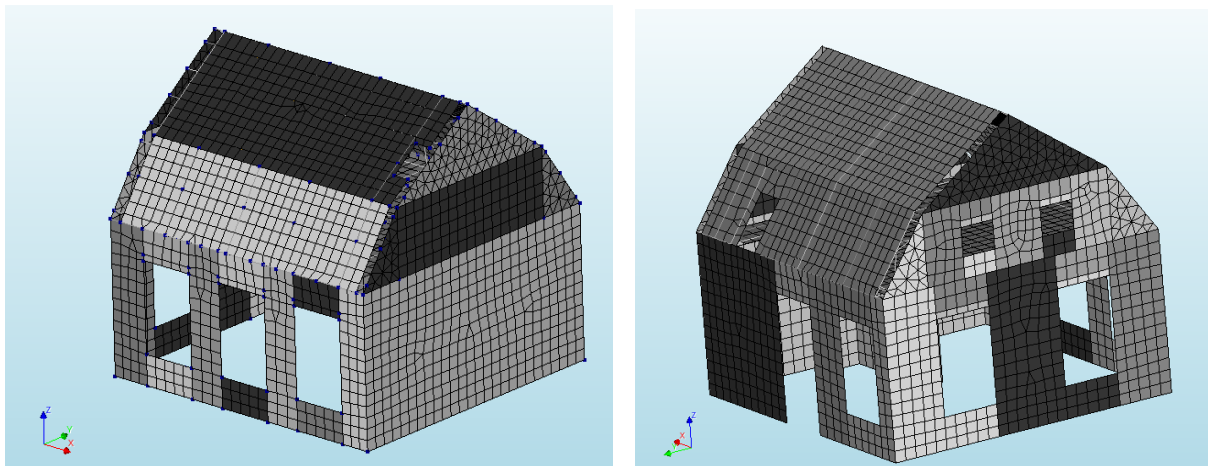


Figure 12: 3D model of LNEC-BUILD-3, variation #01. North-West view (a) and South-East view (b).

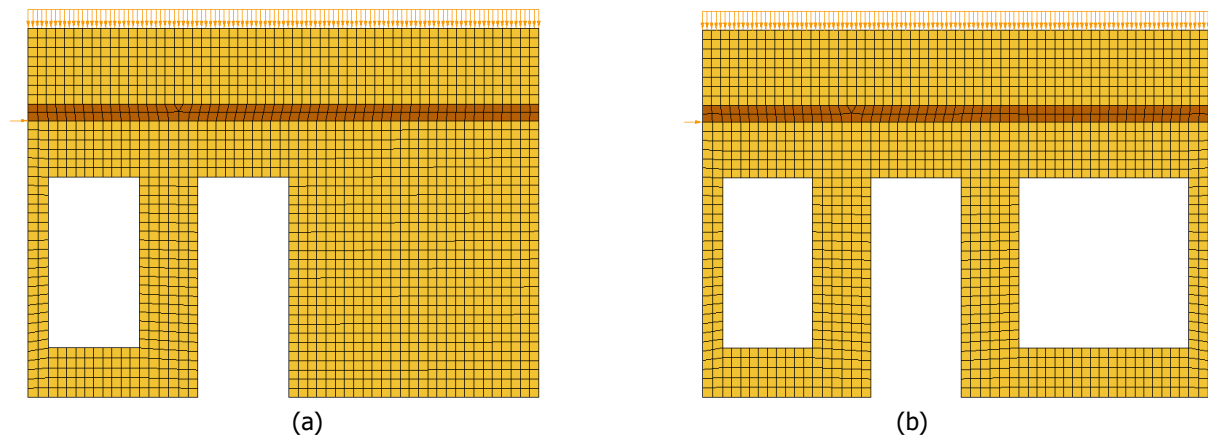


Figure 13. 2D model of a single walls: original pier configuration (34% openings) (a) and configuration with an additional window (67% openings) (b).

5 Comparison of the results

5.1 3D analyses

5.1.1 EUC-BUILD-2

The results of the sixteen 3D analyses performed for the whole building for both the positive and negative loading direction and for both the computational methods are summarised in Table 4 and Table 5, and shown in Figure 14 in terms of equivalent bilinear curve. Refer to Section 3.1.1 for the description of the characteristics of each variation. The average and standard deviation values reported at the bottom of the table are computed assuming a lognormal distribution, that can better approximate the results than a normal distribution. Similarly, the average curves plotted in Figure 14 refer to the lognormal distributions.

Figure 15 shows a comparison between the equivalent lognormal distributions defined for (i) the initial stiffness, (ii) the near collapse displacement, and (iii) the ultimate base shear, computed based on the results of the analyses performed with NLFEA and SLaMA. It should be noted that the columns related to the displacement capacity in Table 4 and Table 5 report only the results for SLaMA because the ultimate capacity of most of the NLFEA was not governed by global in-plane failure mechanisms, rather by local out-of-plane mechanisms that determined numerical instability of the analysis. For this reason, a comparison between the near collapse displacements computed with SLaMA (at global level) and NLFEA (due to local collapses) is not possible. In a similar way, also the distribution of the NC displacements in Figure 15 shows only the values obtained from SLaMA.

Table 4: Results of SLaMA and NLFEA for positive pushover curves for EUC-BUILD-2.

Case #	K_{in} (kN/mm)		d_y (mm)		d_{NC} (mm)		V_u (kN)	
	SLaMA	NLFEA	SLaMA	NLFEA	SLaMA	NLFEA	SLaMA	NLFEA
1P	336.21	494.84	0.300	0.472	49.4	-	100.73	233.4
2P	874.51	467.28	0.125	0.553	54.3	-	109.37	258.3
3P	579.02	547.09	0.167	0.431	46.5	-	96.61	236.1
4P	765.75	529.93	0.123	0.466	48.9	-	94.40	247.0
5P	303.88	486.45	0.310	0.451	54.3	-	94.11	219.4
6P	1085.07	352.69	0.094	0.763	32.7	-	101.62	269.1
7P	342.86	583.38	0.301	0.468	50.9	-	103.10	272.8
8P	336.21	494.84	0.278	0.489	49.4	-	115.28	233.4

Table 5: Results of SLaMA and NLFEA for negative pushover curves for EUC-BUILD-2.

Case #	K_{in} (kN/mm)		d_y (mm)		d_{NC} (mm)		V_u (kN)	
	SLaMA	NLFEA	SLaMA	NLFEA	SLaMA	NLFEA	SLaMA	NLFEA
1N	874.51	467.28	0.125	0.553	29.93	-	109.37	258.3
2N	579.02	547.09	0.167	0.431	33.32	-	96.61	236.1
3N	765.75	529.93	0.123	0.466	29.94	-	94.40	247.0
4N	303.88	486.45	0.310	0.451	46.51	-	94.11	219.4
5N	1085.07	352.69	0.094	0.763	30.11	-	101.62	269.1
6N	342.86	583.38	0.301	0.467	46.56	-	103.10	272.8
7N	414.85	569.61	0.278	0.489	42.71	-	115.28	278.3
8N	145.29	347.77	0.272	0.502	53.53	-	39.50	174.7

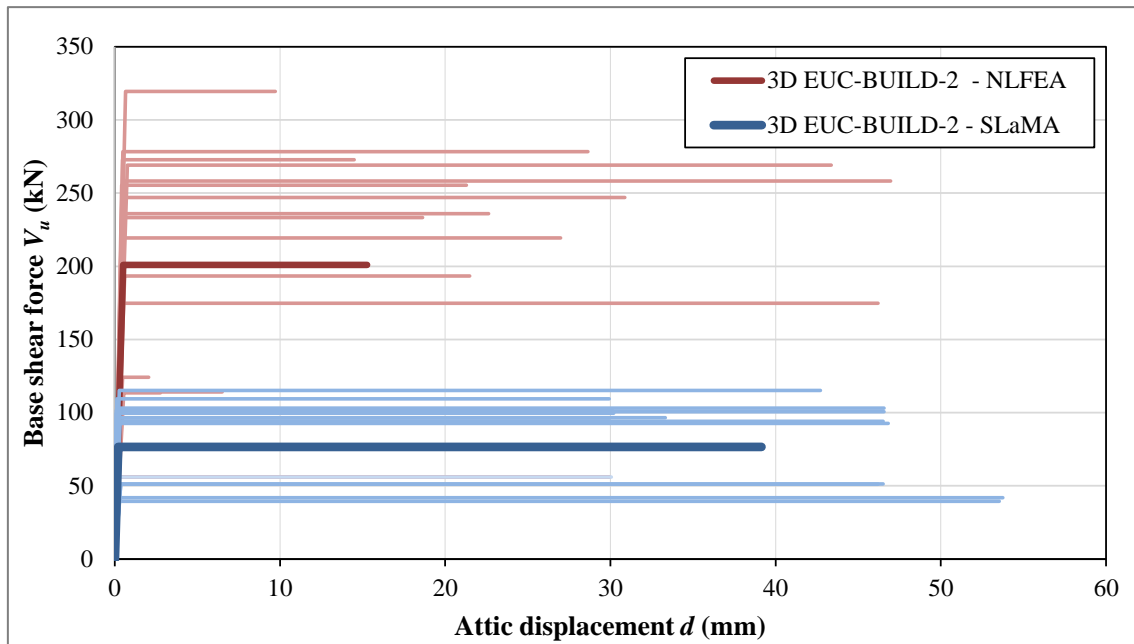


Figure 14: Bilinear curves computed for NLFEA and SLaMA analyses EUC-BUILD-2 (average curves are thicker and darker)

The comparison between the outcomes obtained from the performed analyses, presented in tabular form in Table 6 and in terms of equivalent lognormal distributions in Figure 16, allows for the following observations:

1. Initial Stiffness:

- The plan eccentricity reduces the initial stiffness of the buildings. The variations with no eccentricity had the highest stiffness.
- The initial stiffness is largely affected by the material properties and by the layout of the facades.
- Smaller thickness of the walls and a larger number of openings on the façade reduce the initial stiffness.
- Although differences for the single cases are found between the predictions obtained with SLaMA and with NLFEA, overall similar distributions and average values are found.

2. Yielding Displacement:

- No specific trends are observed. The variation with no eccentricity (#02) has the lowest yielding displacement when SLaMA is used.

3. NC Displacement:

- Larger openings return higher displacement capacity to the structure, because flexure/rocking is the governing failure mechanism.
- As mentioned above, it is not possible to compare the displacement at near collapse obtained with the two methodologies.

4. Base shear capacity:

- Unlike for the initial stiffness, the changes in eccentricity do not affect much the maximum base shear
- The capacity depends on the material parameters; more recent buildings (clay post 1945) have higher capacity.
- SLaMA consistently underestimate the base shear of the buildings with respect to the corresponding NLFEA. A ratio on average of 2.70 a minimum ratio of 1.99 are found.
- The ratio for most of the variations is included between the values 2 and 3, as shown in Figure 16.

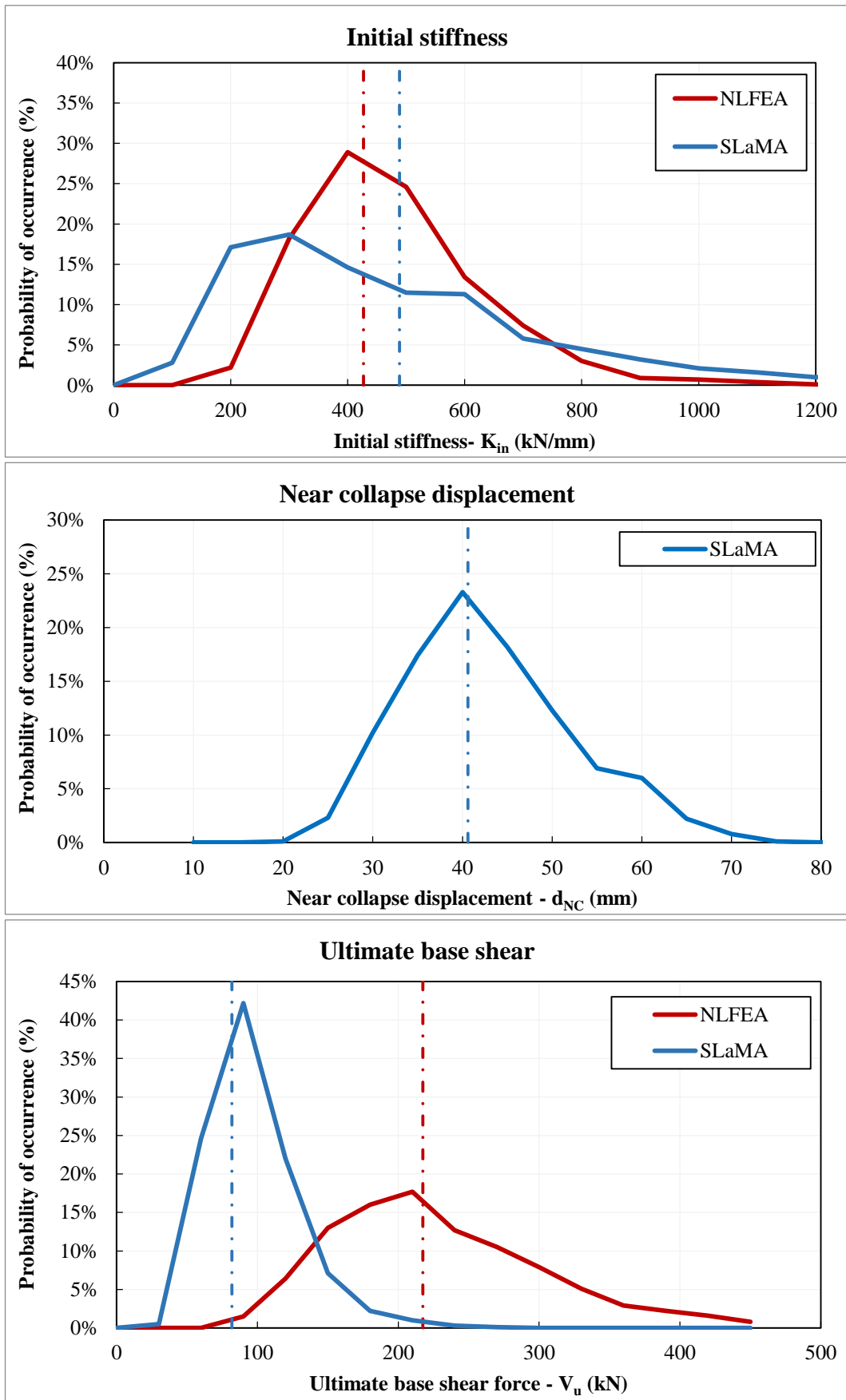


Figure 15: . Comparison between the equivalent lognormal distributions of (i) initial stiffness, (ii) near collapse displacement (for the NLFEA the original data were considered), and (iii) ultimate base shear computed for all the 16 analyses with 3D NLFEA and SLaMA. The dash-dot lines indicate the average values. The probability of occurrence is considered for discrete intervals of 100 kN/mm, 5 mm, 30 kN, respectively.

Table 6: Ratio between the results obtained with the SLaMA and NLFEA for EUC-BUILD-2

Case #	Kin (kN/mm)		dy(mm)		dNC (mm)		Vu (kN)	
	Positive	Negative	Positive	Negative	Positive	Negative	Positive	Negative
1	1.47	0.53	1.57	4.42	-	-	2.32	2.36
2	0.94	0.69	2.59	3.78	-	-	2.44	2.62
3	1.60	0.33	1.46	8.15	-	-	2.33	2.65
4	1.70	1.37	1.56	1.76	-	-	2.65	2.41
5	2.39	2.31	1.85	2.00	-	-	4.42	4.63
6	1.97	0.44	1.40	7.22	-	-	2.76	3.21
7	1.57	0.46	1.27	4.42	-	-	1.99	2.03
8	1.93	0.57	1.15	3.90	-	-	2.23	2.21
Avg	1.27		3.03		-		2.70	

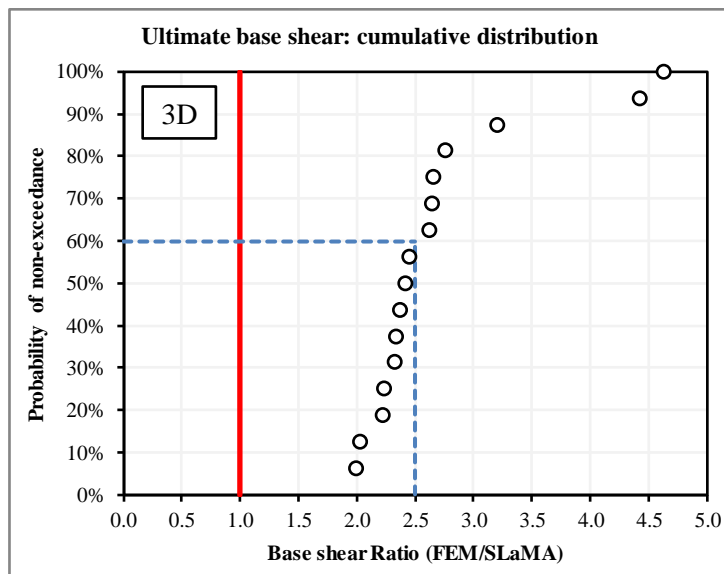


Figure 16: Cumulative distribution functions for the ratio computed for the results of 3D NLFEA and SLaMA analyses in terms of ultimate base shear. For instance, a probability of non-exceedance of 0.6 is obtained for a base shear ratio between the results of NLFEA and SLaMA equal to 2.5 (i.e. the ratio is larger than 2.5 in almost 40% of the cases).

5.1.2 LNEC-BUILD-3

The results of the thirty 3D analyses performed for the whole building for both the positive and negative loading direction and for both the computational methods are summarised in Table 7 and Table 8, and shown in Figure 17 in terms of equivalent bilinear curve. Refer to Section 3.1.1 for the description of the characteristics of each variation. The average and standard deviation values reported at the bottom of the table are computed assuming a lognormal distribution, that can better approximate the results than a normal distribution. Similarly, the average curves plotted in Figure 17 refer to the lognormal distributions.

Figure 18 shows a comparison between the equivalent lognormal distributions defined for (i) the initial stiffness, (ii) the near collapse displacement, and (iii) the ultimate base shear, computed based on the results of the analyses performed with NLFEA and SLaMA. It should be noted that the columns related to the displacement capacity in Table 7 and Table 8.

report only the results for SLaMA because the ultimate capacity of most of the NLFEA was not governed by global in-plane failure mechanisms, rather by local out-of-plane mechanisms that determined numerical instability of the

analysis. For this reason, a comparison between the near collapse displacements computed with SLaMA (at global level) and NLFEA (due to local collapses) is not possible. In a similar way, also the distribution of the NC displacements in Figure 18 shows only the values obtained from SLaMA.

Table 7: Results of SLaMA and NLFEA for positive pushover curves of LNEC-BUILD-3.

Case #	K_{in} (kN/mm)		d_y (mm)		d_{NC} (mm)		V_u (kN)	
	SLaMA	NLFEA	SLaMA	NLFEA	SLaMA	NLFEA	SLaMA	NLFEA
1P	322	621	0.16	0.35	50.3	-	52.0	215.8
2P	324	510	0.16	0.38	49.4	-	50.5	195.7
3P	139	325	0.24	0.45	49.1	-	33.0	144.9
4P	139	267	0.24	0.44	48.8	-	32.9	117.5
5P	320	633	0.18	0.40	49.4	-	57.0	253.6
6P	310	512	0.16	0.38	50.3	-	50.0	196.3
7P	317	698	0.16	0.34	50.3	-	51.2	235.1
8P	900	923	0.13	0.33	32.2	-	112.4	300.5
9P	902	760	0.13	0.34	32.1	-	112.3	259.0
10P	753	485	0.13	0.37	31.9	-	94.4	178.0
11P	768	400	0.12	0.35	31.8	-	94.1	138.2
12P	948	833	0.09	0.33	31.4	-	82.3	272.9
13P	947	689	0.09	0.35	31.3	-	82.2	243.7
14P	419	420	0.13	0.41	31.2	-	54.3	172.3
15P	419	351	0.13	0.39	31.1	-	54.2	137.1

Table 8: Results of SLaMA and NLFEA for positive pushover curves of LNEC-BUILD-3.

Case #	K_{in} (kN/mm)		d_y (mm)		d_{NC} (mm)		V_u (kN)	
	SLaMA	NLFEA	SLaMA	NLFEA	SLaMA	NLFEA	SLaMA	NLFEA
1N	250	609	0.17	0.38	55.1	-	41.6	230.9
2N	256	469	0.16	0.46	55.0	-	41.4	214.0
3N	126	298	0.25	0.45	54.6	-	31.3	134.4
4N	126	251	0.25	0.45	54.4	-	31.2	112.4
5N	288	603	0.19	0.41	55.0	-	53.5	248.2
6N	247	511	0.17	0.42	55.1	-	41.2	214.8
7N	253	697	0.17	0.36	55.1	-	42.2	252.9
8N	943	891	0.15	0.39	32.3	-	136.5	346.8
9N	943	731	0.14	0.42	32.1	-	136.3	305.4
10N	698	466	0.18	0.33	32.1	-	127.5	152.9
11N	711	388	0.18	0.33	31.9	-	127.7	129.3
12N	621	779	0.18	0.45	31.1	-	111.2	347.3
13N	1051	645	0.09	0.43	30.9	-	93.6	274.5
14N	550	407	0.20	0.39	30.9	-	110.1	158.3
15N	779	340	0.12	0.39	30.7	-	95.7	132.0

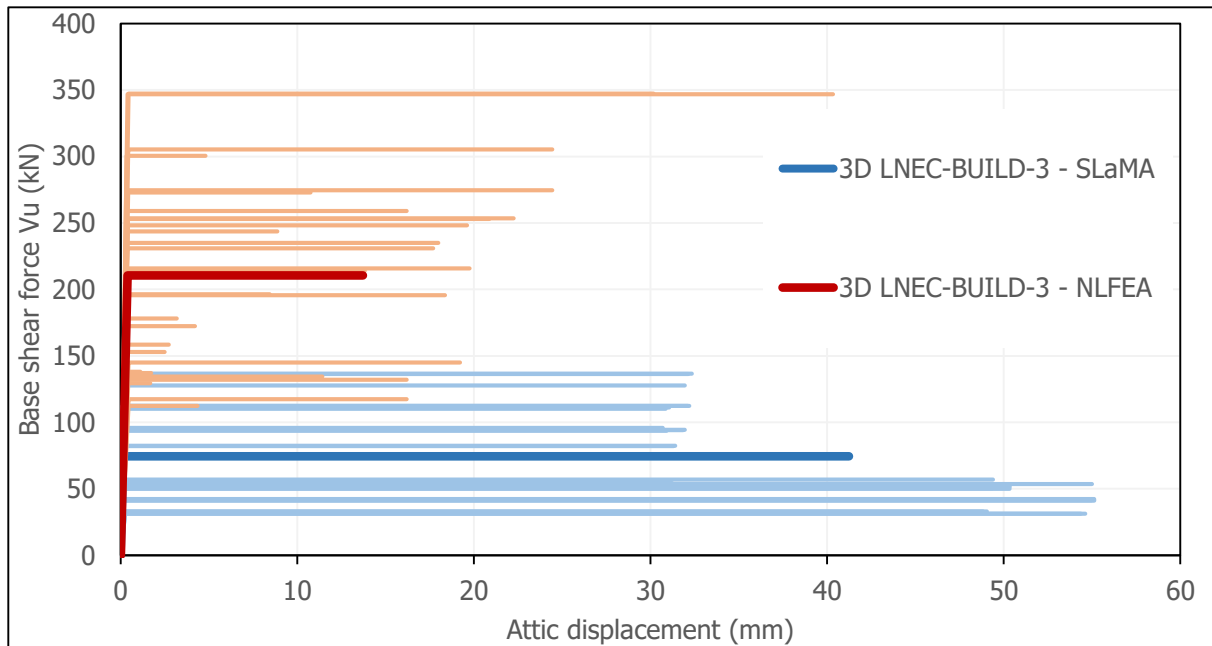


Figure 17: Bilinear curves computed for NLFEA and SLaMA analyses LNEC-BUILD-3 (average curves are thicker and darker)

The comparison between the outcomes obtained from the performed analyses, presented in tabular form in Table 9 and in terms of equivalent lognormal distributions in , allows for remark similar to those observed for the variations of EUC-BUILD-2. In detail:

1. Initial Stiffness:

- The initial stiffness is largely affected by the material properties and by the layout of the facades.
- A larger number of openings on the facade reduces the global stiffness of the building, as expected.
- Also the length of the internal affect the stiffness of the building.

2. Yielding Displacement:

- No specific trends are observed. Large dispersion of the values of the ratio is found.

3. NC Displacement (only for SLaMA):

- Larger openings return higher displacement capacity to the structure, because flexure/rocking is the governing failure mechanism.

4. Base shear capacity:

- The capacity depends on the material parameters; more recent buildings (clay post 1945) have higher capacity.
- SLaMA consistently underestimate the base shear of the buildings with respect to the corresponding NLFEA.
- When observing the cumulative distribution curve (Figure 19), the values of the ratios vary greatly depending on the variation: an average ratio of 3.32 is found, but with a minimum value of 1.01 and a maximum of 5.99.
- Smaller differences are observed for the buildings with only two openings on the façade (variations #8-#15), although large ratios can be found also for those buildings.

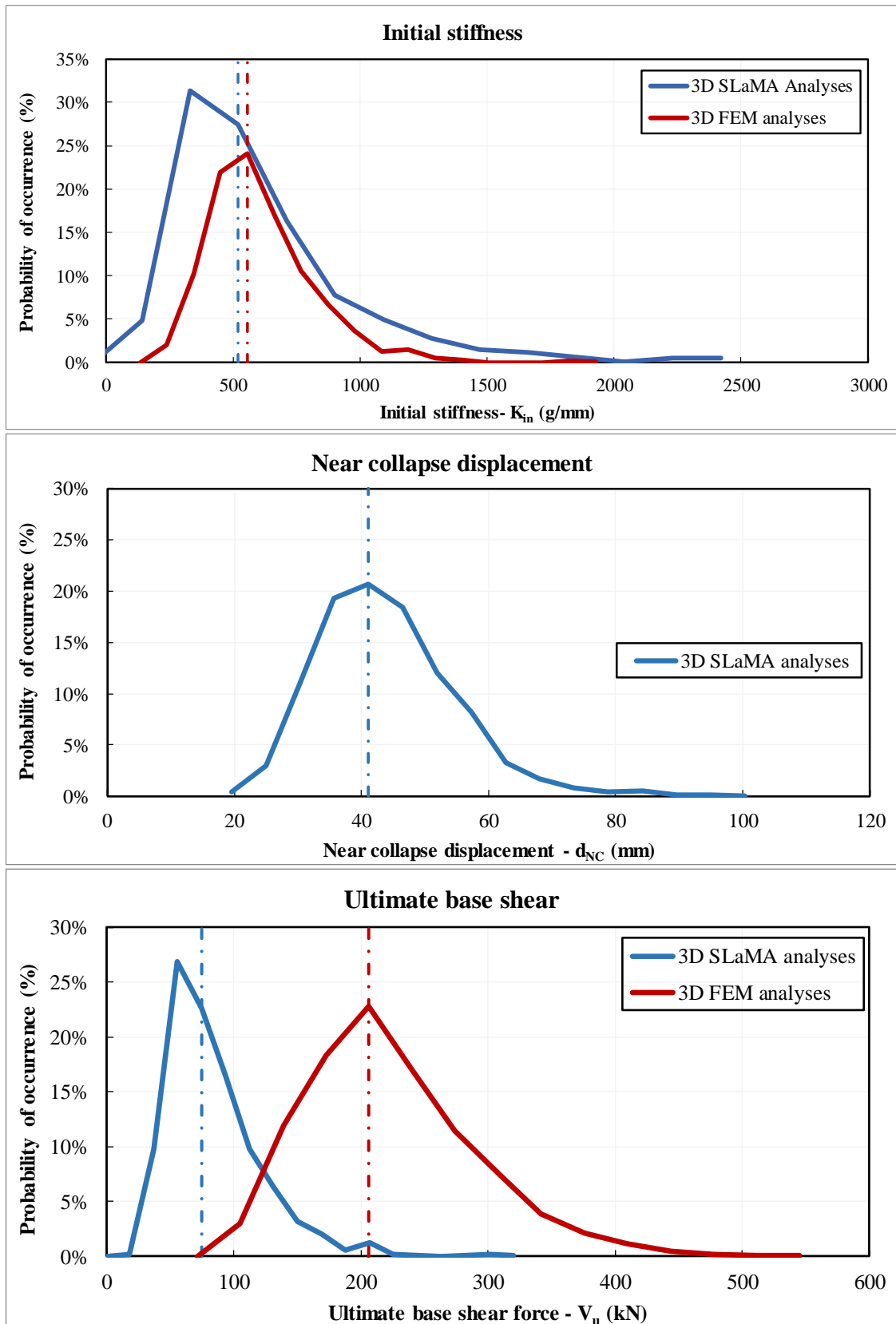


Figure 18: Comparison between the equivalent lognormal distributions of (i) initial stiffness, (ii) near collapse displacement (for the NLFEA the original data were considered), and (iii) ultimate base shear computed for all the 30 analyses with 3D NLFEA and SLaMA. The dash-dot lines indicate the average values. The probability of occurrence is considered for discrete intervals of 10 kN/mm, 5 mm, 10 kN, respectively.

Table 9: Ratio between the results obtained with the SLaMA and NLFEA for LNEC-BUILD-3

Case #	NLFEA/SLaMA							
	K_{in} (kN/mm)		d_y (mm)		d_{NC} (mm)		V_u (kN)	
	Positive	Negative	Positive	Negative	Positive	Negative	Positive	Negative
1	1.93	2.44	2.15	2.28	-	-	4.15	5.55
2	1.57	1.83	2.47	2.82	-	-	3.88	5.16
3	2.34	2.37	1.88	1.82	-	-	4.40	4.30
4	1.92	1.99	1.86	1.81	-	-	3.57	3.60
5	1.98	2.09	2.25	2.22	-	-	4.45	4.64
6	1.65	2.06	2.38	2.53	-	-	3.93	5.21
7	2.20	2.75	2.09	2.18	-	-	4.59	5.99
8	1.03	0.95	2.61	2.69	-	-	2.67	2.54
9	0.84	0.78	2.74	2.89	-	-	2.31	2.24
10	0.64	0.67	2.93	1.79	-	-	1.89	1.20
11	0.52	0.55	2.82	1.86	-	-	1.47	1.01
12	0.88	1.26	3.77	2.49	-	-	3.31	3.12
13	0.73	0.61	4.08	4.78	-	-	2.97	2.93
14	1.00	0.74	3.16	1.94	-	-	3.17	1.44
15	0.84	0.44	3.02	3.16	-	-	2.53	1.38

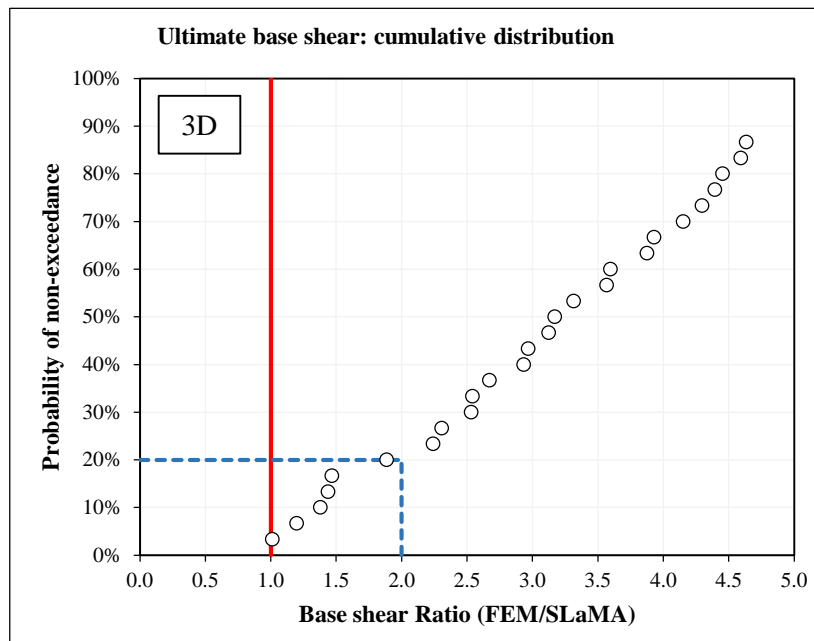


Figure 19: Cumulative distribution functions for the ratio computed for the results of 3D NLFEA and SLaMA analyses in terms of ultimate base shear. For instance, a probability of non-exceedance of 0.2 is obtained for a base shear ratio between the results of NLFEA and SLaMA equal to 2 (i.e. the ratio is larger than 2 in almost 80% of the cases).

5.1.3 All 3D analyses: ultimate base shear

This section summarises the results of all the 3D analyses performed focusing on the ultimate base shear, since it is the parameter for which the largest differences between the results of SLaMA and NLFEA emerge, as described in the previous sections. It can be observed that:

- All the values of the ultimate base shear predicted with a NLFEA are larger than those obtained by the corresponding SLaMA.
- The average base shear capacity and the distributions defined with SLaMA and NLFEA is similar for both the buildings, as shown in Figure 20.
- Although the lognormal distributions look similar for the two buildings, the analysis of the individual variations reveal great differences. This is reflected in the cumulative distribution functions.
- The cumulative distribution functions for the ratios computed between the predictions obtained with NLFEA and with SLaMA differs greatly between the two buildings (Figure 21): for most (80%) of the variations of EUC-BUILD-2 the ratio is comprised between 2.0 and 2.7, and a clear trend can be observed. Conversely, the ratios for LNEC-BUILD-3 are almost uniformly distributed from a minimum value of 1.0 up to a maximum value larger than 4.5.

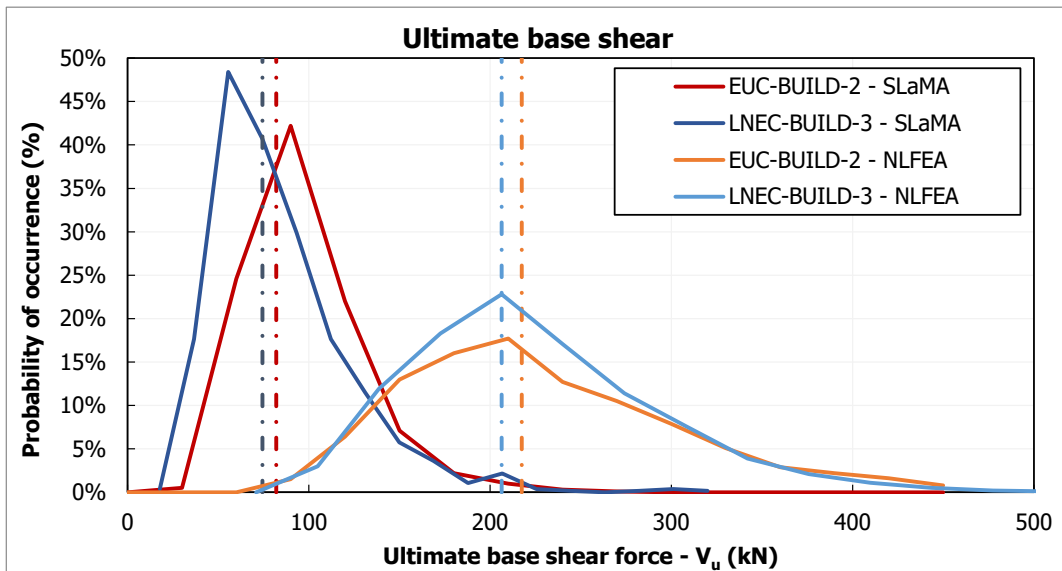


Figure 20. Comparison between the equivalent lognormal distributions of the ultimate base shear computed for all the 46 analyses with 3D NLFEA and SLaMA. The dash-dot lines indicate the average values.

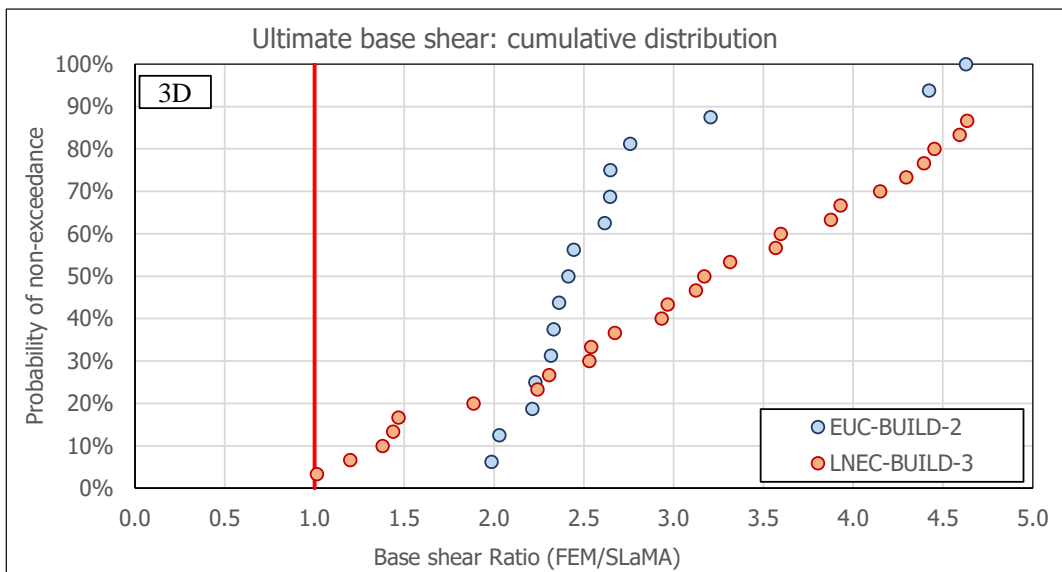


Figure 21. Cumulative distribution functions for the ratio computed for the results of all the 3D NLFEA and SLaMA analyses in terms of ultimate base shear.

5.2 2D analyses

As described in section 3.2, variations of the East façade of the EUC-BUILD-2 building is considered. Given the lower computational effort, for the 2D analyses all the variations are combined systematically and a large total number of combinations is then obtained (576 combinations are analysed).

The differences between the outcomes obtained with NLFEA and SLaMA analyses are compared. Specific attention is devoted to the peak base shear, since this is the parameter where the largest discrepancies between SLaMA and NLFEA analyses emerged for the 3D analyses of the buildings.

Figure 22 shows a comparison between the equivalent lognormal distributions of (i) initial stiffness, (ii) near collapse displacement (for the NLFEA the original data were considered), and (iii) ultimate base shear computed for all the analyses with NLFEA and SLaMA. Table 10 and Table 11 report the ratio between the values of ultimate base shear computed with NLFEA and the SLaMA for each single variation, for the positive and the negative loading direction, respectively.

The following is observed:

1. Similar values of the **initial stiffness** (both in terms of mean values and distributions) are obtained for the computation methods. This result is in line with what was reported in section 5 for the 3D analyses.
2. Unlike the results for the 3D structures, the NLFEA were able to run up to large deformations of the facades (in fact, the out-of-plane failure, which limited the global capacity of the complete structures, cannot occur for 2D analyses of walls). The **near collapse displacements** of the NLFEA are limited by the global drift limits recommended in Table G.2 of NPR 9998 for most of the analyses in case of observed ductile mechanism. The value recommended for such type of mechanisms is higher than the mean value obtained from the SLaMA analyses. The SLaMA calculations are therefore, on average, conservative (the difference, -22%, can be accepted). This can be observed in Figure 22. Similar to the case of the terraced houses [6], the global drift limit defined for ductile mechanisms seems to be properly calibrated.
3. Large differences are found between the **base shear** computed according to SLaMA and NLFEA. The median ratio is larger than 2, as shown in below. Although a large dispersion of the results is observed, the base shear computed with NLFEA is always larger than that computed with SLaMA, with a maximum ratio larger than 5.
The smaller differences are obtained for configurations C5 and C6, which have the largest opening percentages. This result differs from the outcomes of the analyses of building LNEC-BUILD-3, where the smaller differences were observed for walls with piers having a lower aspect ratio.

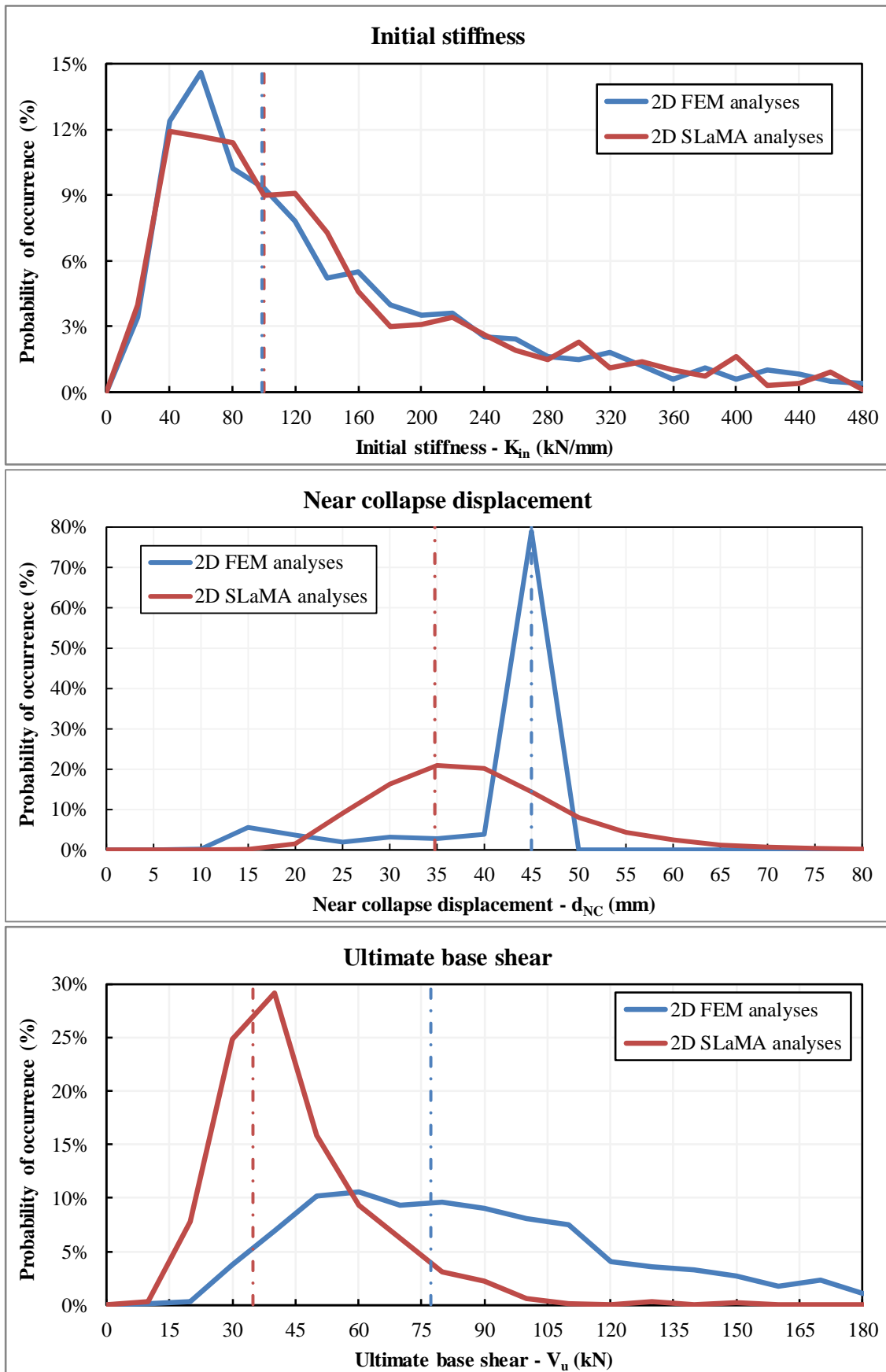


Figure 22: Comparison between the equivalent lognormal distributions of (i) initial stiffness, (ii) near collapse displacement (for the NLFEA the original data were considered), and (iii) ultimate base shear computed for all the 576 analyses with 2D NLFEA and SLaMA. The dash-dot lines indicate the average values. The probability of occurrence is considered for discrete intervals of 10 kN/mm, 5 mm, 10 kN, respectively.

Table 10: Ratio between the values of ultimate base shear computed with NLFEA and the SLaMA for each single variation, for the positive loading direction (red/green background for large/small values, respectively).

MAX BILINEAR FORCE - POSITIVE [kN]		HS												SS																																			
		CL1				CL2				T1				T2				CL1				CL2				T1				T2																			
		DW	SW	DW	SW	DW	SW	DW	SW	DW	SW	DW	SW	DW	SW	DW	SW	DW	SW	DW	SW	DW	SW	DW	SW	DW	SW	DW	SW	DW	SW	DW	SW																
C1	P	2.277	1.963	2.472	1.952	2.977	2.319	2.971	2.293	2.895	2.205	2.836	2.129	3.525	2.473	3.512	2.477	2.818	2.391	3.169	2.406	3.677	2.717	3.633	2.732	3.674	2.485	3.669	2.467	4.390	3.100	4.350	3.053	2.202	1.933	2.495	1.929	2.970	2.228	2.953	2.258	2.655	1.984	2.642	1.969	3.279	2.335	3.273	2.346
	MD	2.070	2.378	1.824	2.332	1.697	1.856	1.692	1.856	3.313	2.579	3.333	2.547	3.821	3.001	3.818	3.011	2.615	2.877	2.314	2.877	2.120	2.128	2.119	2.131	4.196	3.173	4.180	3.198	5.091	3.632	5.088	3.681	2.000	2.308	1.773	2.350	1.624	1.852	1.622	1.834	3.020	2.428	3.009	2.442	3.610	2.739	3.623	2.750
	UC	2.024	1.540	1.860	1.532	2.171	1.767	2.169	1.813	1.977	1.638	1.941	1.649	2.318	1.878	2.308	1.864	2.622	1.837	2.418	1.870	2.785	2.114	2.805	2.093	2.703	2.091	2.709	2.085	3.219	2.345	3.227	2.305	1.945	1.461	1.809	1.482	2.163	1.731	2.080	1.743	1.858	1.544	1.867	1.537	2.232	1.838	2.218	1.829
C2	P	2.240	1.957	2.519	1.971	3.150	2.411	3.174	2.402	2.917	2.212	2.934	2.209	3.760	2.513	3.737	2.507	2.866	2.375	3.132	2.368	3.811	2.787	3.788	2.774	3.792	2.706	3.723	2.756	4.760	3.173	4.776	3.161	2.103	1.829	2.338	1.903	2.962	2.244	2.952	2.243	2.530	1.941	2.511	1.945	3.264	2.350	3.248	2.352
	MD	1.943	1.600	1.951	1.607	2.200	1.745	2.204	1.741	2.470	2.550	2.471	2.543	2.231	2.184	2.229	2.157	2.410	1.932	2.411	1.932	2.727	2.105	2.722	2.101	3.306	3.216	3.304	3.016	2.797	3.027	2.786	2.067	1.819	1.516	1.838	1.501	2.061	1.663	2.065	1.662	2.309	2.402	2.306	2.431	2.030	2.080	2.028	2.067
	UC	1.493	1.363	1.493	1.363	1.558	1.391	1.558	1.391	1.534	1.865	1.533	1.864	1.599	1.912	1.595	1.912	1.445	1.866	1.641	1.864	1.641	1.951	1.682	1.950	1.683	2.078	2.361	2.076	2.360	2.444	2.203	2.445	2.445	1.444	1.326	1.442	1.328	1.506	1.353	1.505	1.352	1.423	1.774	1.420	1.772	1.484	1.810	1.481

CL, ..., C6 = geometry conditions as described in section 4.2
HS and SS = high sprandreis and short sprandreis
MD = modal proportional distributed loads; UD = mass proportional distributed loads; UC = mass proportional loads

Table 11: Ratio between the values of ultimate base shear computed with NLFEA and the SLaMA for each single variation, for the negative loading direction (red/green background for large/small values, respectively).

MAX BILINEAR FORCE - NEGATIVE [kN]		CL1						CL2						HS						CL1						CL2						SS																		
		T1			T2			T1			T2			T1			T2			T1			T2			T1			T2			T1			T2															
		DW	SW	UD	DW	SW	UD	DW	SW	UD	DW	SW	UD	DW	SW	UD	DW	SW	UD	DW	SW	UD	DW	SW	UD	DW	SW	UD	DW	SW	UD	DW	SW	UD																
C1	N	MD	2.015	1.736	1.996	1.721	2.199	2.000	2.175	2.017	2.272	1.779	2.248	1.757	2.879	1.864	2.838	1.845	2.548	2.116	2.530	2.110	3.243	2.456	3.175	2.458	3.053	2.295	3.026	2.259	3.882	2.711	3.839	2.680	1.897	1.634	1.901	1.639	2.045	1.744	2.044	1.742	1.895	1.617	1.902	1.599	2.545	1.732	2.530	1.724
		MD	1.591	1.959	1.606	1.946	1.525	1.460	1.515	1.412	2.954	2.214	2.935	2.210	3.585	2.624	3.625	2.646	2.044	1.959	1.606	1.946	1.525	1.460	1.515	1.412	2.954	2.214	2.935	2.210	3.585	2.624	3.625	2.646	2.044	1.959	1.606	1.946	1.525	1.460	1.515	1.412	2.954	2.214	2.935	2.210	3.585	2.624	3.625	2.646
		UC	1.542	1.931	1.517	1.838	1.463	1.352	1.489	1.384	2.598	1.989	2.604	1.985	3.311	2.369	3.251	2.412	1.542	1.931	1.517	1.838	1.463	1.352	1.489	1.384	2.598	1.989	2.604	1.985	3.311	2.369	3.251	2.412	1.542	1.931	1.517	1.838	1.463	1.352	1.489	1.384	2.598	1.989	2.604	1.985	3.311	2.369	3.251	2.412
C2	N	MD	1.536	1.251	1.531	1.250	1.928	1.455	1.920	1.484	1.549	1.322	1.535	1.315	1.903	1.548	1.882	1.532	1.911	1.506	1.911	1.504	2.311	1.767	2.342	1.773	2.167	1.665	2.153	1.668	2.585	1.940	2.572	1.909	1.539	1.260	1.550	1.264	1.831	1.436	1.832	1.439	1.687	1.316	1.683	1.300	1.911	1.567	1.866	1.566
		MD	1.539	1.260	1.550	1.264	1.831	1.436	1.832	1.439	1.687	1.316	1.683	1.300	1.911	1.567	1.866	1.566	1.539	1.260	1.550	1.264	1.831	1.436	1.832	1.439	1.687	1.316	1.683	1.300	1.911	1.567	1.866	1.566	2.583	2.115	2.524	2.132	3.520	2.385	3.516	2.392	3.051	2.352	3.057	2.333	3.965	2.517	3.930	2.564
		UC	3.190	2.559	3.169	2.532	4.429	3.102	4.362	3.076	3.971	2.977	4.002	2.911	5.085	3.462	5.017	3.482	3.190	2.559	3.169	2.532	4.429	3.102	4.362	3.076	3.971	2.977	4.002	2.911	5.085	3.462	5.017	3.482	2.366	1.995	2.364	1.997	2.876	2.408	2.867	2.327	2.563	2.068	3.345	2.323	3.366	2.306		
C3	N	MD	1.464	1.284	1.464	1.284	1.666	1.408	1.663	1.404	1.961	1.510	1.953	1.404	1.762	1.880	1.749	1.871	1.914	1.596	1.915	1.594	2.133	1.720	2.130	1.717	2.790	2.739	2.732	2.452	2.405	2.437	2.390	1.464	1.284	1.464	1.284	1.666	1.408	1.663	1.404	1.961	1.510	1.953	1.404	1.762	1.880	1.749	1.871	
		MD	1.410	1.227	1.419	1.227	1.626	1.366	1.625	1.363	1.810	1.962	1.799	1.973	1.633	1.752	1.625	1.748	1.410	1.227	1.419	1.227	1.626	1.366	1.625	1.363	1.810	1.962	1.799	1.973	1.633	1.752	1.625	1.748	1.644	1.499	1.644	1.497	1.710	1.559	1.666	1.997	1.665	1.994	1.752	1.625	1.748			
		UC	2.048	1.791	2.048	1.789	2.136	1.873	2.132	1.873	2.267	2.510	2.265	2.504	2.412	2.633	2.410	2.627	1.992	2.048	1.791	2.048	1.789	2.136	1.873	2.132	1.873	2.267	2.510	2.265	2.504	2.412	2.633	2.410	2.627	1.579	1.455	1.579	1.452	1.508	1.562	1.924	1.559	1.924	1.627	1.992				

CL1, ..., C6 = geometry conditions as described in section 4.2

HS and SS = high sprandreils and short sprandreils

MD = modal proportional distributed loads; UD = mass proportional distributed loads; UC = mass proportional loads

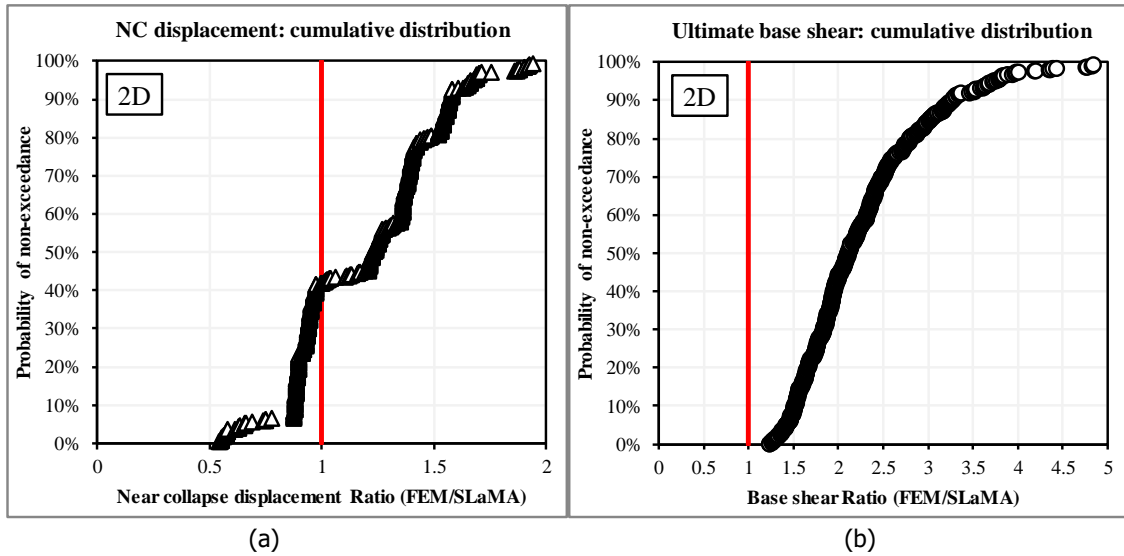


Figure 23: Cumulative distribution functions for the ratio computed for the results of 2D NLFEA and SLaMA analyses: near collapse displacement (a) and ultimate base shear (b).

Finally, the influence of the different parameters on the ratio between the values of Near Collapse displacement and the Ultimate Base Shear computed for the 2D NLFEA and SLaMA analyses, respectively, is analysed and shown in Figure 24 and Figure 25. Figure 24 makes use of radar charts that highlight the parameters for which larger differences between the two computational methods are observed for different groups of analyses. Figure 25 shows the cumulative distribution functions computed for different groups of analyses that differ for only one parameter: different materials (Clay before and after 1945) (a); high and short spandrels (b); different material properties for the timber floor (c); double and single wythe walls (d); number and position of the opening in the façade (e); opening rate of façade (f). In general, the parameters do not influence the computation of the NC displacement, whereas larger differences are found for the ultimate base shear. Specifically:

- The material properties for masonry and timber do not influence the ratio;
- Larger differences are found with short spandrels, because SLaMA is not able to describe appropriately the partial clamping effect that those elements give at top of the piers (but they get, for such short spandrels, that the piers work as cantilever beams); on the other hand, the NLFEA can adequately describe the force redistribution that occurs until the spandrels crack.
- Larger differences are found with larger opening ratios and when the position of the openings determine more slender piers. This is likely due to the relevant effect of the load redistribution that occurs after the failure of one element.
- Larger differences are found for double-wythe walls. However, in this case no specific reason was found to explain the difference.

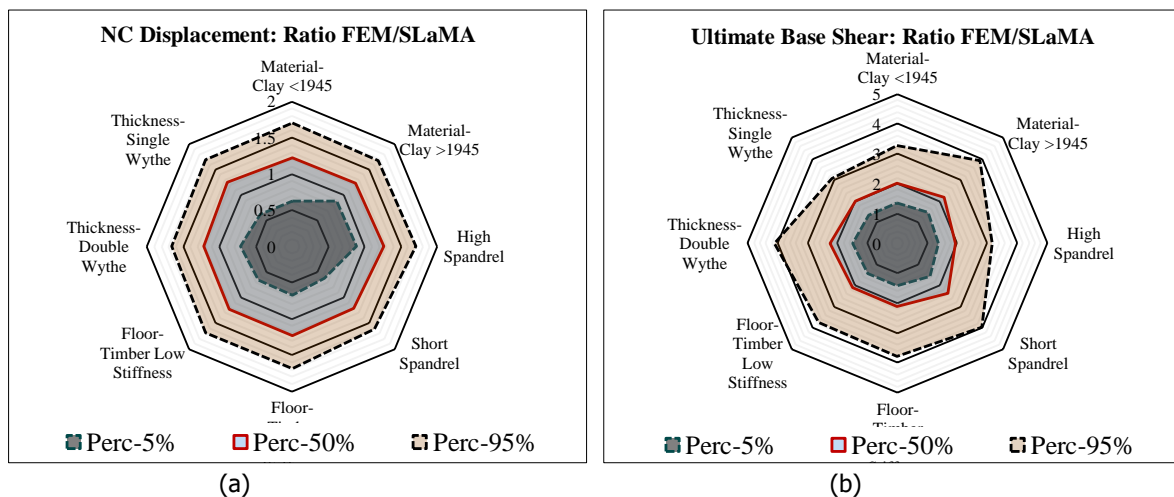


Figure 24: Influence of the different parameters on the ratio NLFEA/SLaMA of 2D analyses for the near collapse displacement (a) and the ultimate Base Shear (b)

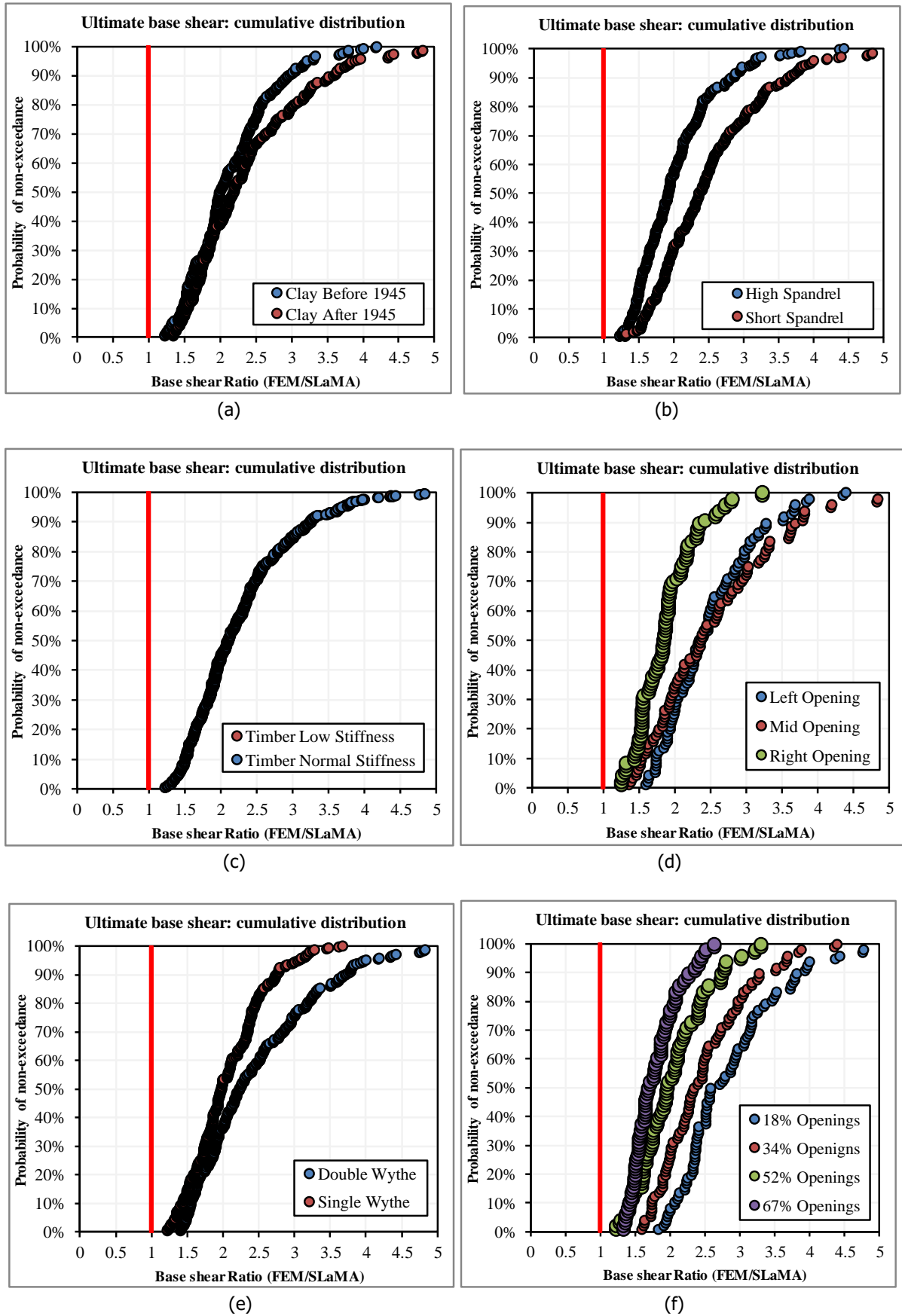


Figure 25: Cumulative distribution functions for the ratio computed for the results of NLFEA and SLaMA analyses.

6 Conclusions

The work described in the current document aims at the calibration of simplified models against more sophisticated nonlinear finite element analyses (NLFEA) for nonlinear pushover (NLPO) analyses for detached houses.

The proposal document consider a large number of NLPO analyses performed on variations of buildings EUC-BUILD-2 and LNEC-BUILD-3. In total 46 3D analyses of the buildings and 576 analyses of single facades have been performed. This large number of analyses allowed for the following observations:

1. As regards the **initial stiffness**:
 - SLaMA and NLFEA provide on average similar predictions of the initial stiffness for both 3D and 2D analyses (both distributions and mean values are similar).
 - It is largely affected by the material properties and by the layout of the facades.
 - The plan eccentricity reduces the initial stiffness of the buildings.
2. With respect to the **yielding displacement**:
 - No specific trends are observed for any of the group of variations (3D for EUC-BUILD-2 and LNEC-BUILD-3, and 2D analyses).
 - Overall, large differences can be found, as for the base shear capacity (see below).
3. Relative to the **NC displacement**:
 - For the 3D analyses it is not possible to compare the displacement at near collapse obtained with the two methodologies SLaMA and NLFEA, because in the latter case the analyses stop before a global collapse is reached due to local out-of-plane (OOP) failure of the walls.
 - For the 2D analyses the OOP collapse cannot occur, and a comparison is possible. In this case, the displacements of most of the NLFEA are limited by the global drift limits recommended in Table G.2 of NPR 9998. The value recommended for such type of mechanisms is higher than the mean value obtained from the SLaMA analyses (+22%).
 - Similar to the case analysed for the terraced houses, the global drift limit defined for ductile mechanisms seems to be properly calibrated also for the walls of the detached houses.
4. Finally, with respect to the **base shear capacity**:
 - SLaMA consistently underestimate the base shear of the buildings with respect to the corresponding NLFEA, for both 3D and 2D analyses: in none of the 622 analyses the peak base shear predicted by SLaMA is higher than that obtained by the NLFEA.
 - Large variation of the differences are found. Depending on the group of analyses, the median ratio computed between the base shear computed based on NLFEA and SLaMA varies between 2.2 and 3.3.
 - If a correction factor 1.5 would multiply the base shear computed with the SLaMA analyses, the corrected base shear would be anyhow smaller than that obtained with NLFEA for approximately 90% of both the 2D and 3D analyses.

Based on the conclusions stated above, when the SLaMA method is used to define the capacity of a building having characteristics in line with those considered in this study (reported in Sections 2 and 3, as well as in [1]), it is suggested to apply no correction factor to the initial stiffness and the near collapse displacement capacity.

With respect to the ultimate base shear, although SLaMA consistently underestimates the results of NLFEA it is complex to recommend the use of a correction factor due to the large dispersion of the ratios computed (with variations from 1.01 up to 5.99). If a factor equal to 1.5 is used to multiply the base shear computed with the SLaMA analyses, the corrected base shear would be anyhow smaller than that obtained with NLFEA for approximately 90% of both the 2D and 3D analyses.

These results are overall similar to those obtained for the study performed for terraced houses, although in that case the application of a correction factor equal to 1.5 would provide conservative results in the 95% of cases with respect to the corresponding NLFEA.

References

- [1] Messali, F. (2019). Cross-validation and calibration of simplified methods for different building typologies. TU Delft Proposal, Final version, 24 September 2019
- [2] Graziotti, F., Tomassetti, U., Rossi, A., Marchesi, B., Kallioras, S., Mandirola, M, Fragomeli, A., Mellia, E., Peloso, S., Cuppari, F., Guerrini, G., Penna, A., Magenes, G. (2016). Shaking table tests on a full-scale clay-brick masonry house representative of the Groningen building stock and related characterization tests. Report EUC128/2016U, Eucentre, Pavia, IT
- [3] Kallioras S, Correia AA, Marques AI, Bernardo V, Candeias PX, Graziotti F. LNEC-BUILD-3: An incremental shake-table test on a Dutch URM detached house with chimneys. EUCENTRE Technical Report EUC203/2018U, EUCENTRE, Pavia, Italy; 2018. Available at www.eucentre.it/nam-project
- [4] Kallioras, S., Guerrini, G., Tomassetti, U., Peloso, S., & Graziotti, F. (2018). Dataset from the dynamic shake-table test of a full-scale unreinforced clay-masonry building with flexible timber diaphragms. Data in brief, 18, 629-640.
- [5] NEN, Nederlands Normalisatie Instituut (2018). NPR 9998:2018 nl. Beoordeling van de constructieve veiligheid van een gebouw bij nieuwbouw, verbouw en afkeuren - Geïnduceerde aardbevingen - Grondslagen, belastingen en weerstanden. Delft, the Netherlands (in Dutch)
- [6] Messali, F., Longo, M. (2019). Calibration of a mechanism-based method against NLFEA for NLPO analyses of URM terraced units. Delft University of Technology. Report number 01, Version 01, 02 December 2019

